Physics – Uspekhi **62** (5) 450 – 464 (2019)

REVIEWS OF TOPICAL PROBLEMS PACS numbers: **12.15.** – y, **13.66.** – a, **29.20.** – e

Experiments at the ILC linear collider: expected physical results

A G Drutskoy

DOI: https://doi.org/10.3367/UFNe.2018.07.038394

Contents

Abstract. The current status of the International Linear e^+e^- Collider project (ILC) planned in Japan is presented. The physical research program proposed at the ILC is discussed, with special attention on the measurements that are possible at a collision energy of 250 GeV and expected statistics of ~ 2 ab^{-1}. These parameters are planned at the first stage of the construction of the collider, where the proposed center-of-mass energy will be limited to 250 GeV. The technical characteristics of the ILC accelerator facility and planned International Large Detector (ILD) are briefly reported.

Keywords: International Linear e^+e^- Collider, experimental tests of the Standard Model, Higgs boson, coupling constants, rare decays, top quark

1. Introduction

The construction of the International Linear e^+e^- Collider (ILC) in Japan is of critical importance to further progress in the area of particle physics. This is a large-scale, technically complicated project, which requires large financial resources and the participation of several thousand scientists from all over the world in the framework of international collaboration. In 2013, detailed information at the ILC was published in the project proposal (Technical Design Report), which encompassed the design of the proposed collider [1], the development of detectors [2], and elaboration of the physical research program [3]. More than 1000 scientists and engineers from laboratories and universities from all over the world, including Russia, participated in the preparation of this document. The last five years have seen tremendous work to further develop all ILC components. At this stage, the technical level of project preparation is unprecedentedly high.

Proposed initially was the construction of the ILC [1] with a center-of-mass energy in a range of 250–500 GeV, with the potential to increase it to 1000 GeV and electron and positron beam polarizations $\mathbf{P}(e^-, e^+) = (-0.8, 0.3)$. The collider length was planned at about 31 km, power consumption at 230 MW, and estimated cost at about 8 bln dollars. Recently the Japanese physical community came up with the idea of limiting the energy to 250 GeV at the first construction stage, which will significantly reduce the collider cost and size. If the ILC project is approved by the Japanese government, its implementation will commence in the near future.

The idea of constructing a linear e^+e^- collider was first proposed by Tigner in 1965 [4]. Then this topic was developed in Ref. [5]. The practical possibilities for the implementation of the linear e^+e^- collider project had been considered in different countries for many years. In particular, under broad discussion were projects in the USA (Next Linear Collider, NLC), Japan (Japan Linear Collider, JLC), and Germany (Teraelectronvolt Energy Superconducting Linear Accelerator, TESLA). Especially deeply and thoroughly elaborated was the TESLA project [6], which implied the possibility of collider operation not only in the standard e^+e^- collision mode, but also in the e^-e^-,$e\gamma$, and $\gamma\gamma$ collision modes after some technical collider modifications. An extensive program of topical physical investigations [7–10] was developed for the TESLA, and the possibility of operating in different modes would have permitted a significant broadening of the spectrum of experimental measurements. Unfortunately, the TESLA project was not approved. Also discussed was the possibility of constructing a linear e^+e^- collider in Dubna. The results of all these developments were integrated and substantially used in the preparation of the ILC project in Japan. Apart from the ILC project, the possibility of

A G Drutskoy Lebedev Physical Institute, Russian Academy of Sciences, Leninskii prosp. 53, 119991 Moscow, Russian Federation;
National Research Nuclear University MEPhI,
Kashirskoe shosse 31, 115409 Moscow, Russian Federation
E-mail: Drutskoy@lebedev.ru

Received 19 February 2018, revised 19 July 2018
Uspekhi Fizicheskikh Nauk **189** (5) 478 – 493 (2019)
DOI: https://doi.org/10.3367/UFNr.2018.07.038394
Translated by E N Ragozin

constructing a Compact Linear e^+e^- Collider (CLIC) with an energy of 380–3000 GeV at CERN is presently under consideration [11, 12]. Proposed recently was a project for a Circular electron positron Collider (CepC) in China [13, 14] with an energy of 250 GeV. Furthermore, at CERN, a discussion was started about the possibility of constructing a giant Future Circular Collider (FCC) with a perimeter of the order of 100 km, whose first stage is intended for e^+e^- beam collisions with a total energy of $\sim$ 350 GeV.

It was earlier hoped that it would be possible to discover new superheavy particles beyond the framework of the Standard Model (SM) in ATLAS (A Toroidal LHC ApparatuS) and CMS (Compact Muon Solenoid) experiments at the Large Hadron Collider (LHC) at CERN. Then, on determining the basic properties of these particles, it would be possible to study them in greater detail on a linear collider, which might call for rather high beam energies. Very close interplay between experiments at the LHC and the ILC was contemplated, so that the data obtained on one collider would complement and direct the research direction vector on the other one.

However, no new heavy particles have been observed at LHC experiments. As a result, in recent years, the proposed program of research on linear colliders has substantially shifted towards precision studies of the known heavy particles: the Higgs boson, the top quark, and W and Z bosons. This correction of plans somewhat divided the research areas: at the LHC the emphasis is placed on the searches for new particles, while the ILC is contemplated for the precision measurement of the known heavy particles. There nevertheless remain several areas in which the contribution of both colliders is required for achieving the needed accuracy, in particular in the measurement of Higgs boson coupling constants.

The particles, processes, and theoretical conceptions Beyond the Standard Model (BSM) are often referred as New Physics. New Physics may show up not only in direct observations of new particles and phenomena, but also in the deviation of the properties of the known particles from those predicted by the SM. It is theoretically hypothesized that heavy particles should have large coupling constants with the particles of New Physics and, accordingly, New Physics may especially markedly manifest itself as a contribution of virtual effects in the processes with the participation of the Higgs boson or the top quark.

Therefore, today, there is no clear demand for the construction of linear colliders with record high beam energies. To study the Higgs boson in the $e^+e^- \to ZH$ reaction, it is necessary to reach a center-of-mass energy of about 240 GeV and an energy of about 370 GeV for pair top-quark production. The W- and Z-boson production threshold is even lower. However, it is noteworthy that of major interest is an energy range of 500–550 GeV, where the three heavy particles may be produced simultaneously. This will enable measurements of several important parameters, in particular the $t\bar{t}H$ coupling constants and the HHH Higgs self-coupling constants.

As a result of the existing situation, the ILC conception was reconsidered. It was suggested that the ILC be constructed with an energy of 250 GeV at the first stage, making it possible to reduce its cost and size by a factor 1.5–2.0 in comparison with the version with the highest energy of 500 GeV. In doing so, it is necessary to retain the possibility of increasing the collider length and beam energies in the future. At the first stage, it is planned to accumulate an integrated luminosity of $\sim 2\,\mathrm{ab}^{-1}$, which will permit the measuring accuracy of Higgs boson parameters expected at the LHC to be significantly improved. A similar suggestion about a step-by-step increase in beam energy is being considered at CERN: it is suggested that the initial energy of the projected linear e^+e^- CLIC be limited to 380 GeV, which would significantly reduce the cost and size of this collider.

In view of the high cost of the ILC project, for the project to be approved, it is critically important to propose an actual and well developed program of topical physical investigations. The program of research on linear e^+e^- colliders elaborated to date is primarily aimed at studying the Higgs boson and the top quark. This is significantly different from the program executed at the LHC and largely complements it. An important feature of the linear e^+e^- collider is that heavy particles will be produced in a rather large proportion of events for a very low background level, which will permit their detailed study. For instance, the Higgs boson should be produced on the linear collider in 1% of events, which will provide the possibility of studying in detail decays of the Higgs boson and its properties proceeding from a data set which is one–two orders of magnitude larger than that achievable at the LHC even after its upgrade. If an energy of 350 GeV is achieved at the ILC, it will be possible to study the properties of top quarks in detail. Precision measurement of W- and Z-boson parameters is also an important experimental task. Should new heavy particles up to 400 GeV in mass be discovered at the LHC, it would be possible to study the properties of these new particles with a high accuracy on the linear collider with sufficiently high beam energies.

In this review, we outline the program of future physical investigations at the e^+e^- ILC. Various aspects of the planned investigations have been considered in several reviews [16–20]. At present, two detectors are planned for construction at the ILC [2]: the International Large Detector (ILD) and the Silicon Detector (SiD). Although the physical research programs for these detectors are very similar, the results of investigations outlined below are based mostly on ILD simulations. Those problems that can be solved at an energy of 250 GeV are considered in greater detail. However, investigations possible at a higher energy are also discussed. This review outlines the technical characteristics of the planned e^+e^- ILC and considers the main parameters of the ILD detector planned for the ILC.

2. Program of physical investigations at the ILC

The main research task on the future linear collider is to study Higgs boson parameters. In this review, the Higgs boson of mass $(125.09 \pm 0.21 \pm 0.11)$ GeV [21], which corresponds to SM predictions, is denoted as H. A remark is in order here. In several papers, especially theoretical ones, the Higgs boson of the Standard Model is denoted by h to distinguish it from the heavy Higgs boson of New Physics denoted by H.

Already at an energy of 250 GeV, the Higgs boson will be produced in the $e^+e^- \to ZH$ channel with a cross section of $\sim$ 300 fb. This will enable obtaining a record large data set comprising of the order of 6×10^5 Higgs bosons with an integrated luminosity of $\sim 2\ \mathrm{ab}^{-1}$ planned for the experiment operation time. One of the main lines of research is the measurement of the branching fractions of various Higgs boson decay channels. This will allow obtaining the Higgs boson coupling constants with leptons, quarks, and vector bosons, which, according to the SM, must be proportional to their masses or, for bosons, to their squared masses. A deviation from this linear dependence would be a direct indication of the manifestation of New Physics.

A special feature of the linear collider is the possibility of model-independent measurements of decay branching fractions and the probability of decay to an unobservable final state. The mass and width of the Higgs boson may be measured with a high accuracy. In view of the large production number of Higgs bosons and a high reconstruction efficiency, it will be possible to carry out the searches for its rare decays. In some models of New Physics, the Higgs boson with a mass of 125 GeV may have a *CP*-odd admixture. Such an admixture may be discovered experimentally on the linear collider at a level of $\sim 10\%$, or the upper limit of its contribution may be obtained.

Pair top-quark production is possible at an energy above 350 GeV. In this case, it is possible to measure the top-quark mass and width with an accuracy an order of magnitude higher than the one presently achieved. Measuring the top-quark coupling to Z bosons and photons is an important task. Also possible is the search for rare decay channels of top quarks. The asymmetry of top-quark production may be measured, and polarization effects in the angular distributions of decay products may be studied. An additional bonus of linear colliders is the possibility of precision measurement of W- and Z-boson parameters. In principle, it is possible to observe the direct production of New Physics particles with anomalously small production cross sections, which are hard to observe at the LHC.

2.1 Reactions involving Higgs boson production

The Higgs boson H will be produced at a center-of-mass energy of 250 GeV in three processes:

1) Higgs boson radiation: $e^+e^- \to HZ$;
2) W bosons fusion: $e^+e^- \to H\nu_e\bar{\nu}_e$;
3) Z bosons fusion: $e^+e^- \to He^+e^-$.

Figure 1 shows tree diagrams of these processes. Figure 2 depicts the center-of-mass energy $\sqrt{s}$ dependence of these channel cross sections simulated assuming that the beam polarizations $\mathbf{P}(e^-, e^+) = (-0.8, 0.3)$. It is noteworthy that electron–positron annihilation is possible only for different helicities of these particles, $e^-_L e^+_R$ or $e^-_R e^+_L$. As a consequence, oppositely polarized beams provide an increase in luminosity. A comparison of the cross sections for the final states for polarized and unpolarized beams was done in Ref. [22]. The values obtained in Ref. [22] are somewhat different from those given in Fig. 2, because they sum up the cross sections for the final states produced by different channels. Beam polarizations are an important experimental factor, because specific SM or New Physics processes may be enhanced by choosing the corresponding combination of beam polarizations. Planned for the ILC at present is the possibility of switching the beam polarizations $\mathbf{P}(e^-, e^+) = (-0.8, 0.3)$ to the opposite ones, $\mathbf{P}(e^-, e^+) = (0.8, -0.3)$.

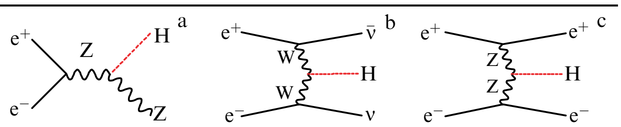

Figure 1. Diagrams describing the reactions $e^+e^- \to ZH$ (a), $e^+e^- \to H\nu_e\bar{\nu}_e$ (b), and $e^+e^- \to He^+e^-$ (c).

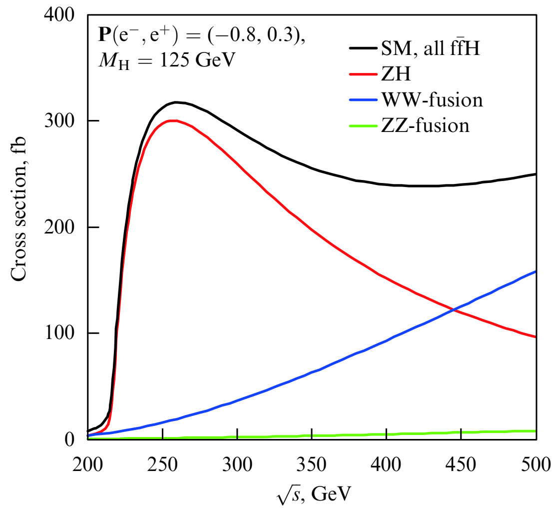

Figure 2. (Color online.) Cross sections for the processes $e^+e^- \to ZH$ (red curve), $e^+e^- \to H\nu_e\bar{\nu}_e$ (blue curve), and $e^+e^- \to He^+e^-$ (green curve) as functions of the beam energies with the proviso that the beam polarizations $\mathbf{P}(e^-, e^+) = (-0.8, 0.3)$. The black curve stands for the total cross section.

As is clear from Fig. 2, at the 250 GeV energy domain, process 1 (Fig. 1a) will prevail with a cross section of about 300 fb, the cross section of process 2 (Fig. 1b) will be 10–15 times smaller, and process 3 (Fig. 1c) will be strongly suppressed: its cross section is further suppressed by about a factor of 10. With increasing energy, the cross section of process 1 decreases and the cross sections of processes 2 and 3 increase, the cross sections for processes 1 and 2 becoming equal in the 450-GeV energy domain.

Studying the Higgs bosons at an energy of 250 GeV requires selecting signal events from background processes with large cross sections, first and foremost from the processes $e^+e^- \to W^+W^-$ and $e^+e^- \to ZZ$. The cross section for the W^+W^- pair production is two orders of magnitude larger than that for the $e^+e^- \to HZ$ process, and the ZZ production cross section is 3–4 times larger. The pair production of fermions also has a large cross section, but these background events are a smaller problem, because their topology may be reliably identified.

With increasing energy, new channels with Higgs boson production will open up, their cross sections being basically available for experimental observations (Fig. 3):

- $E \approx 350$ GeV, $e^+e^- \to HHZ$,
- $E \approx 450$ GeV, $e^+e^- \to HH\nu_e\bar{\nu}_e$,
- $E \approx 480$ GeV, $e^+e^- \to t\bar{t}H$.

As is clear from Fig. 3, the $e^+e^- \to t\bar{t}H$ process cross section may range up to about 1 fb at an energy of 500–550 GeV, so that measuring this channel will call for an accumulation of a large-volume data set. Measuring this cross section will make it possible to measure the $t\bar{t}H$ coupling constant with a high accuracy, which is of paramount importance for identifying New Physics models. A searches for *CP* violation may also be performed in this process. This measurement is discussed in detail in Section 2.5. The $e^+e^- \to HHZ$ channel cross section is still smaller, but in this process it is possible to measure an extremely important parameter: the Higgs boson self-coupling constant. In principle, the Higgs boson self-coupling constant may also be obtained by studying the process $e^+e^- \to HH\nu_e\bar{\nu}_e$, but its

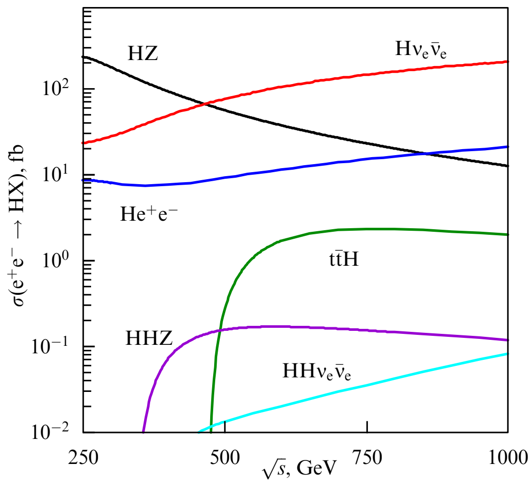

Figure 3. Cross sections for different processes with Higgs boson production as functions of energy in e^+e^- collisions. Unpolarized beams were assumed in the simulation. (Adopted from Ref. [19].)

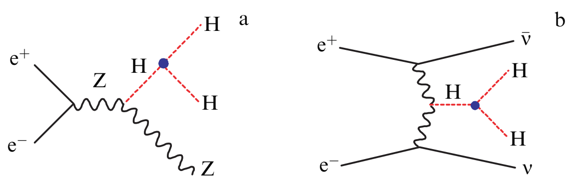

Figure 4. Diagrams describing processes that comprise the triple Higgs vertex: (a) $e^+e^- \to HHZ$ and (b) $e^+e^- \to HH\nu_e\bar{\nu}_e$.

cross section is extremely small. Figure 4 shows the corresponding diagrams with a triple Higgs vertex, which include the Higgs boson self-coupling constant.

2.2 Higgs boson decays

In the first approximation, the Lagrangian describing the interaction of the Higgs boson with fermions, gauge bosons, and the Higgs boson itself may be represented as

$$\mathscr{L} = -g_{\mathrm{Hf\bar{f}}} H\bar{f}f + \delta_V g_{\mathrm{HVV}} HV_\mu V^\mu + \frac{1}{6} g_{\mathrm{HHH}} H^3, \qquad (1)$$

where $V = \mathrm{W}^\pm(\mathrm{Z}^0)$, $\delta_V = 1$ for $V = \mathrm{W}^\pm$ or 1/2 for $V = \mathrm{Z}^0$. The coupling constants are proportional to the corresponding mass or squared mass:

$$g_{\mathrm{Hf\bar{f}}} = \frac{m_{\mathrm{f}}}{v}, \quad g_{\mathrm{H}VV} = \frac{2m_V^2}{v}, \quad g_{\mathrm{HHH}} = \frac{3m_{\mathrm{H}}^2}{v}. \qquad (2)$$

The vacuum average of the Higgs doublet $v = (\sqrt{2}G_{\mathrm{F}})^{-1/2} \approx$ 246 GeV is accurately determined from the Fermi coupling constant G_{F}. The proportionality of the coupling constants to the fermion mass and the squared mass of vector Z and W bosons is the basic prediction in the framework of the SM. Departures from the proportionality will be direct indication of New Physics.

When the Higgs boson mass is accurately known, in the framework of the SM it is possible to calculate the coupling constants and, accordingly, the relative probabilities of Higgs boson decay into different final states (Table 1). In the calculations of electroweak processes, loop corrections are usually small and may be accurately estimated.

Mainly tree diagrams are used to show Higgs boson decays into fermions and vector bosons. However, the Higgs boson decays into gluons, two photons, and $Z\gamma$ may be described only by loop diagrams. Therefore, by analyzing these decays, it is possible to indirectly obtain information about HWW, HZZ, and $\mathrm{Ht\bar{t}}$ coupling constants. It is also noteworthy that the decays $\mathrm{H} \to \mathrm{WW}^*$ and $\mathrm{H} \to \mathrm{ZZ}^*$ may occur only when at least one of the vector bosons is outside of the mass shell.

In the ATLAS and CMS experiments at the LHC, a significance of over 5σ was achieved for the decay channels $\mathrm{H} \to \gamma\gamma$, $\mathrm{H} \to \mathrm{ZZ}^*$, $\mathrm{H} \to \mathrm{WW}^*$, and $\mathrm{H} \to \tau^+\tau^-$, and over 3σ for the $\mathrm{H} \to \mathrm{b\bar{b}}$ channel. The coupling constants measured for these channels agree nicely with the linear dependence on mass expected for the SM. Quite often, introduced for simplicity is the signal strength parameter $\mu = (\sigma\mathcal{B})_{\mathrm{meas}}/(\sigma\mathcal{B})_{\mathrm{SM}}$, equal to the ratio of the observed product of the cross section σ and the branching fraction for some process $\mathcal{B}$ with Higgs boson production to the corresponding value expected from the SM. Results consistent with the SM must yield $\mu = 1$. The combined value of μ, which includes data from both LHC experiments and all significant channels, $\mu = 1.09 \pm 0.07 \pm 0.09$ [21], which demonstrates good agreement between experimental data and the predictions of the SM.

2.3 Measurement of coupling constants, Higgs boson width and mass

Measuring the Higgs boson coupling constants with a high accuracy is the most important task for experiments at the ILC. It is noteworthy that these measurements can be performed at the ILC in a model-independent way. In this case, the measuring accuracy of coupling constants will be higher than that at the LHC, even after its upgrade. Methods of measuring the coupling constants at different energies, in particular at 250 GeV, were considered in Ref. [24].

For a better understanding of the method for measuring the Higgs boson coupling constants, we give in Table 2 the branching ratios for the main channels of Z-boson decay.

For an energy of 250 GeV, different approaches may be employed to determine the total Higgs boson width Γ_{H} and the coupling constants. It is required to measure several products of the cross sections and branching fraction for the following processes:

Table 1. Theoretical estimates* of the main branching ratios for Higgs boson decay channels for $m_{\mathrm{H}} = 125.09$ GeV.

Higgs boson decay, branching ratios, %									
$\mathrm{b\bar{b}}$	$\mathrm{c\bar{c}}$	$\mathrm{s\bar{s}}$	$\tau^+\tau^-$	$\mu^+\mu^-$	WW^*	ZZ^*	gg	$\gamma\gamma$	$\mathrm{Z}\gamma$
58.1	2.88	0.0246	6.26	0.0217	21.5	2.64	8.18	0.227	0.154

* The values were borrowed from Ref. [23]. Also given there are the uncertainties for these theoretical estimates, which range from 1–5%.

Table 2. Experimental measurements* of the main branching ratios for Z-boson decay channels.

Z-boson decays, %						
$\tau^+\tau^-$	$\mu^+\mu^-$	e^+e^-	Hadrons	$b\bar{b}$	$c\bar{c}$	Unobservables
3.37 ± 0.008	3.366 ± 0.007	3.363 ± 0.004	69.91 ± 0.06	15.12 ± 0.05	12.03 ± 0.21	20.00 ± 0.06
* Values borrowed from Ref. [21].						

$$\text{I.}\quad \sigma(\mathrm{HZ})\,\mathcal{B}(\mathrm{Z} \to \mu^+\mu^-) = C_1 g_Z^2\,,$$

$$\text{II.}\quad \sigma(\mathrm{HZ})\,\mathcal{B}(\mathrm{Z} \to \mu^+\mu^-)\,\mathcal{B}(\mathrm{H} \to \mathrm{WW}^*) = \frac{C_2 g_Z^2 g_W^2}{\Gamma_H}\,,$$

$$\text{III.}\quad \sigma(\mathrm{HZ})\,\mathcal{B}(\mathrm{Z} \to \mu^+\mu^-)\,\mathcal{B}(\mathrm{H} \to \mathrm{b\bar{b}}) = \frac{C_3 g_Z^2 g_b^2}{\Gamma_H}\,,$$

$$\text{IV.}\quad \sigma(\mathrm{H}\nu\bar{\nu})\,\mathcal{B}(\mathrm{H} \to \mathrm{b\bar{b}}) = \frac{C_4 g_W^2 g_b^2}{\Gamma_H}\,.$$

Here, g_Z, g_W, and g_b are the HZZ, HWW, and $\mathrm{Hb\bar{b}}$ Higgs boson coupling constants, and C_1, C_2, C_3, and C_4 are constants, which may be accurately obtained by theoretical calculations with an uncertainty of less than 1%.

Measured in process I is the $\mu^+\mu^-$ system mass, as well as the missing mass of this system. The simultaneous determination of the $\mu^+\mu^-$ mass in the Z-boson mass region and of the missing mass in the Higgs-boson mass region makes it possible to unambiguously separate process I and, accordingly, find the number of events and the cross section for the final state HZ. In the example of distribution over the missing mass given in Fig. 5 [20], a dataset with an integrated luminosity of 250 fb^{-1} was assumed in the simulation. Background processes were also simulated, and they are included in the distribution shown in Fig. 5. The ILD detector model was used in the reconstruction of events. The signal is well extracted from the background. Seen on the right side of the picture is a tail related to the radiation in the initial state. For an expected integrated luminosity of ~ 2 ab^{-1}, the uncertainty of measuring the $e^+e^- \to \mathrm{ZH}$ process cross section will be about 1%. Accordingly, the g_Z coupling constant will be determined with the same accuracy. From the formal standpoint, additional reconstruction of the $\mathrm{H} \to \mathrm{ZZ}^*$ decay will permit determining the Higgs boson width, though with a rather low accuracy, because the number of events in this channel is too small.

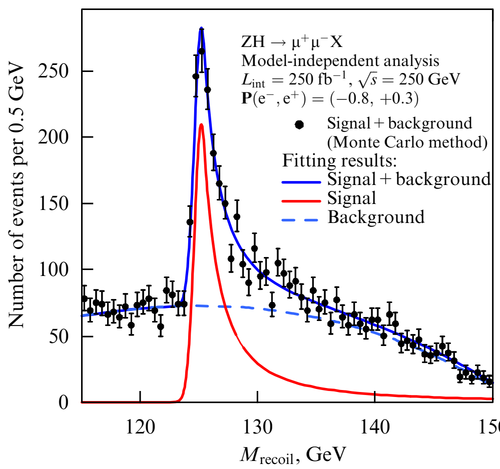

Figure 5. Missing mass distribution to the $\mu^+\mu^-$ system. Simulations were made of the $e^+e^- \to \mathrm{ZH}$ signal process with the subsequent $\mathrm{Z} \to \mu^+\mu^-$ decay for a center-of-mass energy $\sqrt{s} = 250$ GeV and an integral luminosity $L_{\mathrm{int}} = 250\ \mathrm{fb}^{-1}$. (Adopted from Ref. [20].)

The possibility of using the missing mass technique is a significant advantage of the e^+e^- collider. This method permits solving several tasks at once. First, the method provides normalization for determining the branching ratios for various Higgs boson decay channels. Second, it permits measuring the total Higgs boson width. Third, by determining the sum of all exclusive Higgs boson decay channels and comparing it with the inclusive value obtained by the missing mass technique, it is possible to estimate the probability of decay into the invisible final state with an accuracy of about 1%. Last, by applying this method, it is possible to determine the Higgs boson mass with an uncertainty of $\sim$30–40 MeV [25].

Therefore, by using the missing mass technique, it is possible to carry out precision measurements of the Higgs boson mass and width. At present, the combined value of the Higgs boson mass, which includes the results of measurements performed by ATLAS and CMS, is $m_H = 125.09 \pm 0.24(\pm 0.21 \pm 0.15)$ GeV. In the framework of the SM, the Higgs boson width may be predicted with a high accuracy, provided its mass is known. For a mass $m_H = 125.1$ GeV, the width should be 4.2 MeV. An experimental limitation on the Higgs boson width $\Gamma_H < 22$ MeV was indirectly obtained at a confidence level (CL) of 95% in the ATLAS and CMS experiments [26, 27].

As stated above, the total Higgs boson width may in principle be obtained in a model-independent way by measuring process I and the $\mathrm{H} \to \mathrm{ZZ}^*$ decay, but this method does not provide sufficient accuracy. This measurement may be performed more accurately at an energy of 250 GeV by following the method considered in detail in Ref. [24]. This study suggests that g_Z be determined from the measurement of the cross section of process I, then the ratio g_Z/g_W and, accordingly, the g_W value be obtained from the cross section ratio of processes III and IV. Then, for known g_Z and g_W, it is possible to extract the total Higgs boson width from the measurement of the cross section of process II. With the data set for a luminosity of 250 fb^{-1} at an energy of 250 GeV, it is possible to measure the width with an accuracy of $\sim 13\%$ and, with the use of additional channels, an accuracy of $\sim 11\%$ may be achieved [24].

In the opinion of the author of this review, the total Higgs boson width may be measured using another reconstruction method. The proposed method consists of reconstructing the Higgs boson in the $\mathrm{H} \to \mathrm{ZZ}^*$ decay, where the Z boson will be reconstructed in two-jet quark channels, $\mathrm{Z} \to \mathrm{jj}$, in particular, in the case of $\mathrm{b\bar{b}}$ and $\mathrm{c\bar{c}}$ jets, and Z^* will decay in two-lepton channels: $\mathrm{Z}^* \to l^+l^-$, where $l^\pm$ is $\mu^\pm$ or $e^\pm$. The invariant mass m_{jj} of the two jets from the Z-boson decay will have a broad signal distribution. However, to improve the resolution in the Higgs boson mass, use can be made of the mass difference, since the uncertainty of jet parameter measurements is largely reduced in this difference, and the signal should have a smaller width in the distribution over this variable. Using this channel of Higgs boson decay, it is possible to reconstruct about 500 $e^+e^- \to HZ$ events with a luminosity of ~ 2 ab^{-1}. The Higgs boson width may be obtained from the formula $\sigma_{HZ}\,\mathrm{Br}\,(H \to ZZ^*) = C g_Z^4/\Gamma_H$ with the understanding that the constant C may be calculated theoretically and the coupling constant g_Z will be measured with a high accuracy. This method of measuring the Higgs boson width has not been discussed in the literature, although the method of reconstructing the decay $H \to ZZ^*$ in the quark channels of Z and Z^* decays was considered in a somewhat different context in review Ref. [19, Section 5.1]. This method is not employed at the LHC, supposedly due to a strong background, although a two-muon trigger should, in principle, efficiently select such events.

It should be noted that the main objective of coupling constant measurements is to identify deviations of the resultant figures from SM predictions. To simplify calculations, in several papers [3, 19] the coupling constant being determined was expressed in terms of its value in the SM: $g_i = \kappa_i g_i^{\mathrm{SM}}$. In the case of agreement between experimental data and the SM, a complete set of modifier values $\kappa_i = 1$ should be obtained. This approach is commonly referred to as the κ formalism. Several modifiers were measured at the LHC, and their values coincide with unity to within the accuracy of measurements.

Measuring the κ_i modifiers is one of the most important tasks for the ILC. The majority of New Physics models entail deviations of modifier values from unity at a level of several percent, and for some modifiers up to 10%. In this case, specific models will lead to certain specific modifier shifts and thereby leave characteristic 'footprints', by which specific New Physics model may be identified. However, an important factor in this procedure is the modifier measurement accuracy. The coupling measurement accuracy may be significantly improved at the ILC at an energy of 250 GeV (Fig. 6) [28]. As is clear from Fig. 6, the accuracy of determining the majority of coupling constants with the use of combined LHC and ILC data is $\sim 1\%$, while with the use of only the LHC data the uncertainty amounts to at least $\sim 4\%$. In Section 2.4, we dwell in more detail on the New Physics models and modifier-assisted identification.

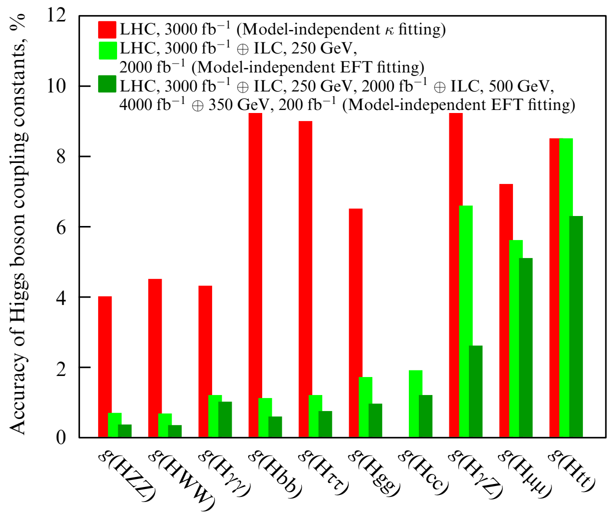

Figure 6. (Color online.) Accuracy of determining Higgs boson coupling constants obtained in the framework of the Effective Field Theory (EFT) [18]. The accuracy estimates obtained by the ATLAS collaboration for the High Luminosity LHC (HL-LHC) for an integral luminosity of 3000 fb^{-1} [28] are compared with the accuracy expected when employing the combination of LHC and ILC measurements, in particular in the accumulation of a luminosity of 2 ab^{-1} in an ILC experiment at an energy of 250 GeV. (Adopted from Ref. [28].)

Unfortunately, the κ formalism is not a universal description method in the case of manifestation of New Physics. A possible approach to identify New Physics models may be realized on the basis of the conception proposed in the framework of the Effective Field Theory (EFT). This approach implies that deviations from the SM predictions may be described with anomalous contributions to the Lagrangian by adding operators dimension-6 [29]. By applying this method for parametrizing the Higgs boson coupling constants, it is possible to show that it would suffice to perform rescaling with κ modifiers to describe the Higgs boson decays into fermions, but this is insufficient to describe the Higgs boson coupling to vector Z and W bosons. For instance, the interaction of the Higgs boson with the Z boson may be described with a Lagrangian describing the contribution of the anomalous tensor interaction:

$$\mathscr{L} = -\frac{m_Z^2}{v}\,(1+\eta_Z)\,HZ_\mu Z^\mu + \frac{\zeta_Z}{2v}\,HZ_{\mu\nu}Z^{\mu\nu}\,. \qquad (3)$$

Here, m_Z is the Z boson mass, and η_Z and ζ_Z are constants which account for the respective contributions of standard and anomalous interactions. Similarly, it is possible to take into account the interaction of the Higgs boson with the W boson. Under this approach, the parametrization of the cross sections and widths assumes a more complicated form. The coefficients in the formula that comprises constants η_Z and ζ_Z will vary in relation to the interaction energy and specific process. In particular, the production and decay of the Higgs boson at an energy of 250 GeV will involve different parametrizations:

$$\sigma(e^+e^- \to HZ) = (c_{\mathrm{SM}})\,(1 + 2\eta_Z + 5.7\zeta_Z)\,,$$
$$\Gamma(H \to ZZ^*) = (c_{\mathrm{SM}})\,(1 + 2\eta_Z - 0.5\zeta_Z)\,. \qquad (4)$$

Here, (c_{SM}) indicates that the terms on the right-hand sides of relations (4) calculated in the framework of the Standard Model are corrected by the corresponding factors, which replace the simplest κ modifiers. An adequate description of the coupling constants in the framework of the Effective Field Theory assumes a more complicated procedure of measurement data processing. The corresponding procedure was proposed in Ref. [29].

2.4 New Physics models

Several New Physics models involve extension of the Higgs sector. The simplest version of extension is proposed by the Minimal Supersymmetric Standard Model (MSSM) [30]. From the standpoint of Higgs sector extension, this model coincides with the two-Higgs-Doublet Model (2HDM). Expected in the framework of this model is the appearance of five Higgs fields corresponding to two *CP*-even scalar particles, light H_1 and heavy H_2, one *CP*-odd particle A^0, and two charged $H^\pm$. It is noteworthy that the light and heavy Higgs bosons are sometimes denoted by h^0 and H^0, respectively. In this case, the light supersymmetric boson H_1 should possess properties similar to those of the SM Higgs boson, which coincide with the properties of the boson with a mass of ~ 125 GeV discovered at CERN. This model will entail a small modification of the SM Higgs boson coupling constants in production and decay due to the contributions both of tree and of loop diagrams. In the framework of supersymmetric models, additional contributions may be due to the loop contributions of supersymmetric particles. There is a variety of these models. In several types of models, in particular, three neutral Higgs bosons mix, which should result in appearance of a *CP*-odd component of the Higgs boson with a mass of 125 GeV.

A broad spectrum of specific models is proposed in the literature in the framework of the general 2HDM approach. Furthermore, there are more structurally complex extensions of the Higgs sector. In particular, Higgs triplet models (HTM) with a still larger set of Higgs fields have been proposed, including those with doubly charged Higgs bosons $H^{++/--}$. Generally speaking, additional heavy Higgs bosons must exist in the framework of these models, but they have not been discovered so far on the LHC. Production of such additional Higgs bosons with weak coupling as the ILC is possible in the processes like

- $e^+e^- \to HA^0$,
- $e^+e^- \to H^+H^-$,
- $e^+e^- \to H^{\pm}W^{\mp}$.

Another common example of the Higgs sector extension is the model of a composite Higgs boson [31, 32]. The most widespread version of this approach is the so-called Little Higgs model (LHM) [33], as well as theories with additional space dimensions (Higher Dimensions) [34]. In the framework of these models, new strong interactions are introduced on an energy scale of the order of 10 TeV. In the LHM, 10 Higgs bosons with masses of several TeV additionally appear, including the light degenerate Higgs boson 125 GeV in mass.

Experimental manifestations of New Physics models may be expected in a variety of measurements. Research in this area was described at length in review Ref. [17]. The most efficient direct method in the searches for New Physics involves measurements of Higgs boson coupling constants. Departures from 125-GeV Higgs boson coupling constants from the SM values are exemplified in Fig. 7 in the framework of different models of New Physics. Furthermore, there are several other parameters which may be indicative of New Physics effects. Among the measurements of such parameters is the determination of the upper limit for the contribution of the *CP*-odd component of the Higgs boson. It is also necessary to search for rare decays of the Higgs boson and its rare production processes. Furthermore, the branching fraction of Higgs boson decay into an 'invisible' final state must be accurately measured in the search for the contribution of a possible decay into new unknown particles. Any deviation from SM predictions would be a direct indication of a contribution from New Physics.

2.5 Measurement of the *CP* parity of the Higgs boson

To measure the contribution of a *CP*-odd admixture to the Higgs boson with a mass of 125 GeV, which is basically possible in New Physics models, we can use only certain production and decay channels. In the majority of processes, spin information either is lost due to hadronization or cannot be extracted. From the practical standpoint, spin analysis is possible in four processes: in the $H \to ZZ^*$ decay with four leptons in the final state; b) in the $e^+e^- \to HZ(l^+l^-)$ process; c) in the decay $H \to \tau^+\tau^-$, where τ-lepton decay products allow obtaining information; d) in the $e^+e^- \to t\bar{t}H$ process, where the top quark decays prior to the onset of hadronization, and so its decay products retain information about the spin configuration of the process.

The $H \to ZZ^*$ decay with four leptons in the final state is the simplest to analyze. However, the number of reconstructed Higgs bosons in this channel will be small at the

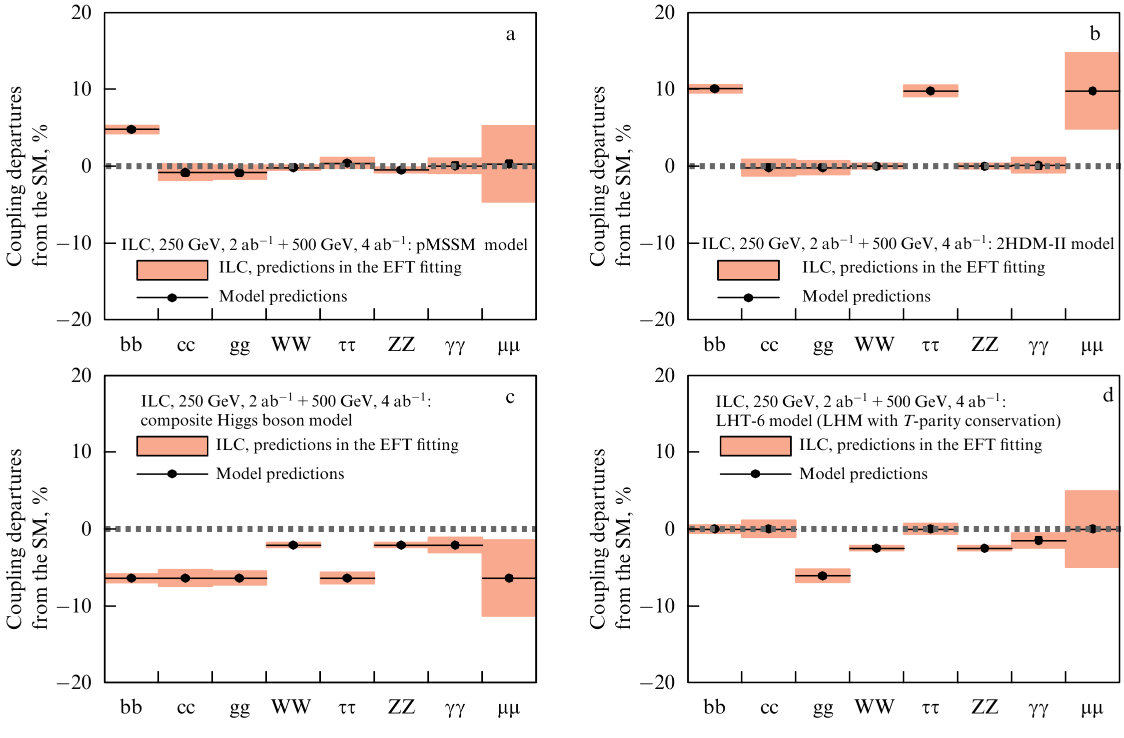

Figure 7. Departures of the Higgs boson coupling constants from the SM predictions for one of the versions of the MSSM (a), 2HDM-II (b), the composite Higgs boson model (c), and little Higgs model (LHM) (d). (Adopted from Ref. [29].)

ILC, and this channel is better suited for studies at the LHC. In addition, it is hard to obtain a quantitative estimate of the CP-odd admixture in this channel due to the following circumstance. In the standard description of this interaction, the CP-even Higgs boson decays into two Z via a tree diagram, while the CP-odd Higgs boson transits to this final state only via strongly suppressed loop diagrams. As a result, the contribution of the CP-odd component is initially suppressed, and so it cannot be determined quantitatively in the $\mathrm{H} \to \mathrm{ZZ}^*$ decay.

Under the EFT approach, the CP-odd contribution to the $\mathrm{H} \to \mathrm{ZZ}^*$ decay may nevertheless range up to several percent, provided that the New Physics processes are introduced in the form of an anomalous contribution [35] as in Eqn (3), which may contain an additional term corresponding to the contribution of a CP-odd tensor component:

$$\mathscr{L} = -\frac{m_Z^2}{v}\,(1 + a_Z)\,HZ_\mu Z^\mu + \frac{b_Z}{2v}\,HZ_{\mu\nu}Z^{\mu\nu} + \frac{\tilde{b}_Z}{2v}\,HZ_{\mu\nu}\tilde{Z}^{\mu\nu}\,, \tag{5}$$

where a_Z provides renormalization, b_Z corresponds to the CP-even tensor component, and $\tilde{b}_Z$ accounts for the CP-odd contribution.

In the analysis of $\mathrm{H} \to \mathrm{ZZ}^*$ decays, use is commonly made of the standard set of angles (Fig. 8a): exit angles of the decay products of Z and Z* in their rest frame, as well as the angle between the decay planes of Z and Z*, which is the most sensitive to the CP-odd admixture to the Higgs boson. An angular analysis of the $\mathrm{H} \to \mathrm{ZZ}^*$ decays with the use of this approach was carried out in the ATLAS [36] and CMS [37] experiments, and upper bounds were obtained at respective confidence levels of 97.8% and 97.6% that the Higgs boson is a pure $J^p = 0^-$ state. However, as noted above, this method does not permit estimating the admixture of the CP-odd component.

The same problem arises with the $\mathrm{e}^+\mathrm{e}^- \to \mathrm{ZH}$ process, where the CP violation also manifests itself at the ZZH vertex, which is described by the loop diagram for the CP-odd component. Nevertheless, as in the case of $\mathrm{H} \to \mathrm{ZZ}^*$ decays, in the framework of the EFT approach the CP-odd component may also make an observable contribution here. As is noteworthy, in the $\mathrm{e}^+\mathrm{e}^- \to \mathrm{ZH}$ channel at the ILC it is possible to reconstruct a large number of events against a low background and, accordingly, achieve a high measuring accuracy for the CP-odd component. The angles sensitive to CP violation in this process are shown in Fig. 8b. The method of measuring the CP-odd admixture in the $\mathrm{e}^+\mathrm{e}^- \to \mathrm{ZH}$ channel in ILC experiments is discussed in Ref. [35].

Potentially, the $\mathrm{H} \to \tau^+\tau^-$ decay is the most efficient way of measuring the CP-odd component of the Higgs boson at the ILC. On the one hand, this decay has a large decay branching fraction. On the other hand, τ-lepton decay products may be employed to measure the spin configuration. To perform the angular analysis, use can be made of the decays $\tau^\pm \to a^\pm \nu_\tau$, where $a^\pm = \pi^\pm, \rho^\pm, \mathrm{a}_1{}^\pm, \mathrm{l}^\pm\nu_\mathrm{l}$, but each specific channel has its own pros and cons.

The Lagrangian for the $\mathrm{H} \to \tau^+\tau^-$ decay may be represented as

$$\mathscr{L} = -\frac{m_\tau}{v}\,H\bar{\tau}\,(\cos\psi_{CP} + \mathrm{i}\sin\psi_{CP}\,\gamma^5)\,\tau\,, \tag{6}$$

where m_τ is the τ-lepton mass and angle ψ_{CP} characterizes the CP-component ratio for the Higgs boson. The zero mixing angle, $\psi_{CP} = 0$, corresponds to a pure CP-even state, and angle $\psi_{CP} = \pi/2$ corresponds to a pure CP-odd state.

As in the case of $\mathrm{H} \to \mathrm{ZZ}^*$ decay, the angle between τ-lepton decay planes is the most sensitive to the measurement of the mixing angle. The existence of an unregistered neutrino in τ-lepton decays complicates the measurement procedure, but fast τ-leptons decay some distance from the primary vertex, making it possible to determine the decay plane by measuring their daughter particles. For the process $\mathrm{e}^+\mathrm{e}^- \to \mathrm{HZ}$, with subsequent $\mathrm{Z} \to \mu^+\mu^-$, $\mathrm{H} \to \tau^+\tau^-$, and $\tau^\pm \to \pi^\pm\nu_\tau$ decays, the parameters of all particles may be determined by measuring the impact parameters of π-mesons and invoking conservation laws [39]. By using this method, it is possible to calculate the angle between the planes and estimate the possible CP-odd component contribution. The authors of Ref. [38] propose the use of modified angle ϕ^*_{CP} between the planes, the distributions in which are appreciably different for the CP-even and CP-odd components (Fig. 9). According to the estimate made in Ref. [39], a set of data accumulated for an integrated luminosity of 2 ab^{-1} at an energy of 250 GeV will permit measuring the mixing angle ψ_{CP} with an accuracy of 4.3°.

The process $\mathrm{e}^+\mathrm{e}^- \to \mathrm{t\bar{t}H}$ may also be employed in the searches for the CP-odd Higgs boson contribution, but measuring this process calls for an energy of at least 500 GeV. A special feature of this process is the possibility of direct observation of CP violation, because three diagrams make contributions to this process (Fig. 10).

The diagram in Fig. 10c comprises the ZZH vertex, which, as discussed earlier, is dominated by the CP-even contribu-

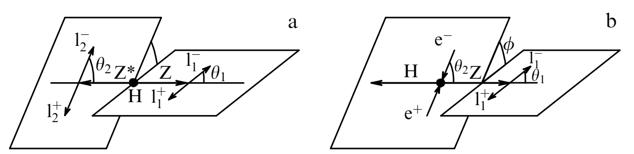

Figure 8. Standard set of angles measured in the $\mathrm{H} \to \mathrm{ZZ}^*$ decay (a) and in the process $\mathrm{e}^+\mathrm{e}^- \to \mathrm{HZ(ll)}$ (b), which are employed in spin analysis: helicity angles θ_1 and θ_2, as well as angle ϕ between the decay planes.

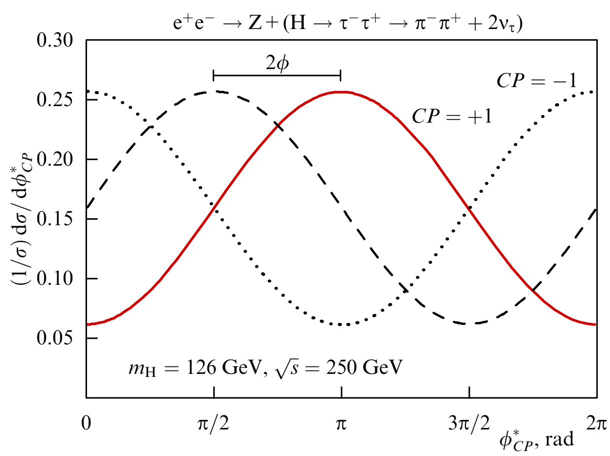

Figure 9. Normalized distribution in the modified angle ϕ^*_{CP} for the process $\mathrm{H} \to \tau^+\tau^- \to \pi^+\pi^- + 2\nu$. The solid, dotted, and dashed curves show the distributions for the CP-even and CP-odd Higgs boson and for their 50-percent mixture, respectively. (Adopted from Ref. [38].)

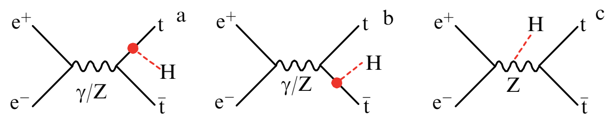

Figure 10. Diagrams describing the $e^+e^- \to t\bar{t}H$ process.

tion. At the same time, the diagrams in Figs 10a and 10b comprise the $t\bar{t}H$ vertex, in which the *CP*-odd contribution is not suppressed. The interference of these diagrams can lead to the manifestation of direct *CP* violation, which may be measured with the help of the normalized triple product:

$$\mathcal{O} = \frac{\mathbf{p}_t(\mathbf{p}_{e^-} \times \mathbf{p}_{\bar{t}})}{|\mathbf{p}_t||\mathbf{p}_{e^-}||\mathbf{p}_{\bar{t}}|}\,, \tag{7}$$

where $\mathbf{p}_t$, $\mathbf{p}_{\bar{t}}$, and $\mathbf{p}_{e^-}$ are the top quark, anti-top quark, and beam electron momenta [40]. Irrespective of the model, the normalized triple product should be equal to zero in the case of *CP*-parity conservation and differs from zero in the case of its violation. Generally speaking, there are other ways to search for *CP* violation in the $e^+e^- \to t\bar{t}H$ process, in particular by measuring the energy dependence of the process cross section or the top- anti-top-quark production asymmetry. However, these methods require exact theoretical predictions for the pure *CP*-even state and are therefore model-dependent. Options for *CP* violation measurements in processes involving top quarks are described in Ref. [41].

It is noteworthy that *CP* violation may also be searched for in the pair top-quark production $e^+e^- \to t\bar{t}$ [41]. In this case, the *CP* violation may be related to the vertex in the loop diagram. The contribution of such diagrams should be small in comparison with the contribution of the main tree diagram and, accordingly, the *CP*-odd component will be small. Despite the difficulty in searching for a small *CP* violation in this process, the high cross section of the process may be a kind of compensation.

2.6 Search for rare decays of the Higgs boson at the ILC

The ILC is often referred to as a Higgs factory. For an integrated luminosity $L_{\rm int} \sim 2$ ab^{-1} accumulated at an energy of 250 GeV, it is possible to obtain a data set comprising approximately 6×10^5 Higgs bosons. Accordingly, this provides a possibility of searching for rare decays with a branching fraction down to $(2-20) \times 10^{-5}$, depending on the signal reconstruction efficiency and the background conditions.

One of the first on the list of rare decays which can be searched for at the ILC is the $H \to Z\gamma$ decay, which is expected to have a branching fraction of $\sim 1.5 \times 10^{-3}$. Unfortunately, the most pure lepton decay modes $Z \to e^+e^-/\mu^+\mu^-$ have a total branching fraction of 6.7×10^{-2}. This makes this search quite difficult in view of the ~ 40 events expected for $L_{\rm int} \sim 2$ ab^{-1}. Accordingly, to increase the number of events, it is necessary to use $Z \to jj$-type two-jet decay modes. These decay modes will markedly increase the number of events but will entail a significant background, which has to be efficiently suppressed. The production of a high-energy photon in the background processes is primarily related to initial state radiation (ISR). In the data set acquisition with $L_{\rm int} = 2$ ab^{-1}, attempts to see the $H \to Z\gamma$ decay will supposedly meet with success, but to do so, some methodical problems have to be solved.

The next on the list is the $H \to \mu^+\mu^-$ decay, which has a branching fraction of 2.17×10^{-4}. For a full data set, the expected number of events amounts to ~ 100, which should provide the opportunity to observe this decay [42]. Background processes are associated primarily with the high-energy muon productions in $Z \to \mu^+\mu^-$ and $W^\pm \to \mu^\pm\nu$ decays, but the high momentum resolution of the ILC detectors would be able to extract the signal from the background. It is pertinent to note that this decay is of major interest in connection with observations of deviations of the branching fraction of lepton B-meson decays from SM predictions, which have been widely discussed in recent times. These deviations are treated as a manifestation of lepton universality violation. Also of interest in this connection is the searches for the $H \to e^+e^-$ decay, which has, in the framework of the SM, a branching fraction that is approximately 40,000 times lower than the decay to two muons.

The branching fraction of the $H \to J/\psi\gamma$ decay estimated in the framework of the SM amounts to $\sim 2.5 \times 10^{-6}$ [43], and so rare a decay is impossible to see even in the final data set. However, there is good reason to search for this process, because the contributions of New Physics may raise its probability.

In addition to the searches for Higgs boson rare decays allowed in the framework of the SM, it is necessary to search for as broad a list as possible of decays forbidden in the SM. Among these processes is the decay $H \to \tau^\pm\mu^\mp$ with lepton flavor violation (LFV). This process may have an experimentally achievable branching fraction in the framework of a number of New Physics models. The rather stringent limitations imposed on these models may be obtained from the existing measurements of the upper limits of $\tau \to \mu\gamma$ decays, but in Higgs boson decays the situation may be much different.

It is also necessary to search for the decay $H \to b\bar{s}$, whose branching fraction in the SM is estimated at a level of 10^{-7}, but this value may significantly grow in several New Physics models, particularly in the New Physics models in the Higgs sector. This is because in several models the limitations on the $H_2 \to b\bar{s}$ heavy Higgs boson decays are absent or are artificially introduced. Experimentally, the searches for $H \to b\bar{s}$ decays is technically complicated. The search for Higgs boson decays to lighter final states with lepton or quark flavor violations is possible, but these decays are strongly suppressed according to theoretical estimates.

2.7 Top quark studies

Since it has been suggested to limit the total energy to 250 GeV at the first stage of ILC operation, here we give only a brief description of possible top-quark research on e^+e^- colliders. As is evident from Fig. 11, to study top quarks requires attaining a total energy of at least 380 GeV. However, the peak $e^+e^- \to t\bar{t}$ process cross section equal to ~ 700 fb is reached near the threshold. Processes with single top-quark production are formally possible at lower energies, for instance $e^+e^- \to t\bar{c}$, but the probabilities of these processes are very low. The properties of top quarks may be studied not only in the main channel $e^+e^- \to t\bar{t}$ but also in the processes $e^+e^- \to t\bar{t}H$ and $e^+e^- \to t\bar{t}Z$, but their cross sections are much smaller, and the beam energies should be appreciably higher (see Fig. 11). The dominant decay channel for experimental top-quark studies is $t \to Wb$, where the W boson may be reconstructed both in the lepton mode with an unrecorded neutrino and in the two-jet hadronic mode.

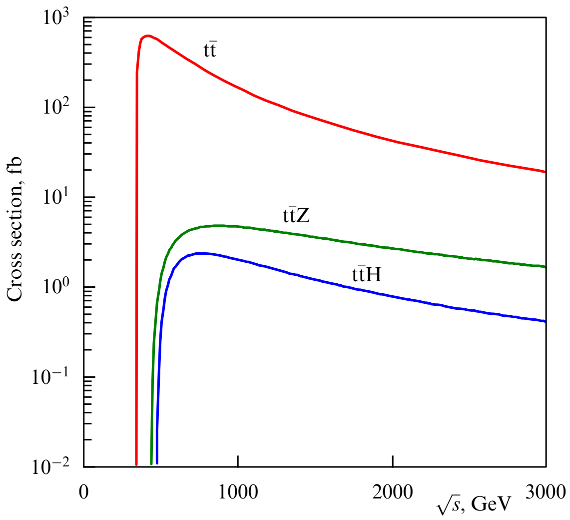

Figure 11. Cross sections for top-quark production processes as functions of e^+e^--collider energy [44] obtained in WHIZARD 2 generator assisted simulations.

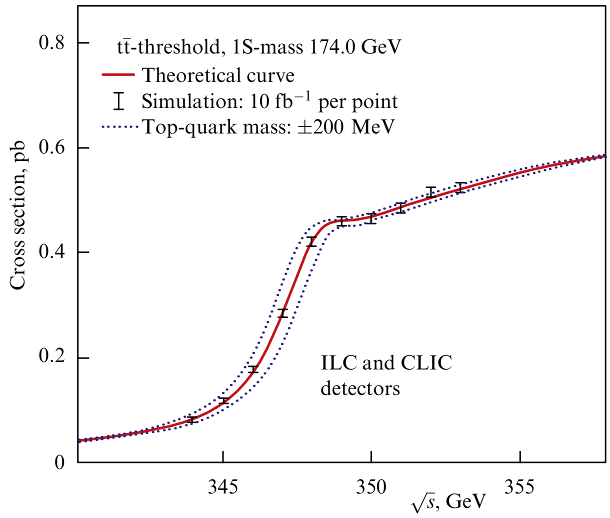

Figure 12. Simulated comparison of the experimental measurement of the $t\bar{t}$-pair production cross section with theoretical curves [47]. Cross section measurements are proposed at 10 points in energy near the threshold for an integrated luminosity of about 10 fb^{-1} at each point. The top-quark mass in the simulations is equal to 174 GeV.

According to estimates, background processes may be significantly suppressed in the reconstruction of top quarks.

The top quark is the heaviest experimentally observed object, which largely underlies the significant interest in it. Precise measurement of its parameters is of significant theoretical importance. In particular, the top-quark mass is the fundamental parameter of electroweak theory and its value has a strong effect on the calculated loop corrections for different processes. However, the interpretation of the notion of the top-quark mass is quite unambiguous.

There are a number of theoretical top-quark mass definitions. In particular, quite often the top-quark mass is theoretically represented as the value of a mass pole, but this definition entails significant uncertainties of the order of the coupling constant Λ_{QCD} of quantum chromodynamics. The top-quark mass nay be alternatively defined by the position of the peak in the 1S resonance mass or as the $\overline{MS}$ mass defined in the renormalization scheme. These two theoretical definitions are slightly different, however the estimated difference being under 10 MeV [45].

Experimentally, the top-quark mass is measured by reconstructing decay products on hadron colliders. In principle, this method yields the mass value built into Monte Carlo simulations, which is hard to relate to theoretical top-quark mass definitions. The uncertainty expected in the conversion of the resultant value to the theoretical one may range up to 1 GeV. Experimental systematic uncertainties on hadron colliders are slightly less than 0.5 GeV today, with the prospect of lowering them to 0.2 GeV for a high luminosity at the LHC in the future [46]. Another method of measuring the top-quark mass on hadron colliders is to compare the experimental $t\bar{t}$-pair production cross section with the results of theoretical calculations including the top-quark mass. This method is also substantially model-dependent and entails large uncertainties.

The top-quark mass may be obtained with a much higher accuracy by measuring the $t\bar{t}$-pair production cross section on e^+e^- colliders at several energies near the production threshold. This method permits obtaining a top-quark mass which agrees more precisely with theoretical mass definitions and has a significantly smaller uncertainty. An experimental accuracy of ~ 20 MeV may be obtained by measuring 10 points near the threshold for an integrated luminosity of about 10 fb^{-1} at each point [46, 47]. Figure 12 shows the simulation of such a comparison of experimental data with theoretical curves.

The precision of theoretical predictions is an important factor in the employment of this top-quark mass measuring method. Recent times have seen significant progress in this direction. Reference [48] outlines the $t\bar{t}$-pair production cross sections calculated as functions of e^+e^- collider energy in the framework of NLO (next-to-leading order), NNLO (next-to-NLO), and N^3LO (next-to-next-to-NLO) approximations. The α_s measurement inaccuracy introduces a significant uncertainty into these calculations, but the accuracy of this parameter should significantly improve during the linear collider construction period. We note that the technique of measuring the $e^+e^- \to t\bar{t}$ process cross section makes it possible to obtain a figure for the top-quark mass close to the theoretical interpretation in the 1S resonance mass. The total theoretical uncertainty of this method, which comprises the inaccuracy of calculations and the uncertainty as to the relation between the experimental and theoretical values, amounts to ~ 50 MeV [44, 46].

The top-quark width is also an important parameter of the theory. Direct width measurements on hadron colliders, which is methodically complicated, entails large uncertainties. The width may be obtained indirectly by measuring the cross section for single top-quark production. According to the Particle Data Group (PDG) collaboration [21], the average value $\Gamma_t = 1.41^{+0.19}_{-0.15}$ comprises hadron collider measurements performed with the use of both methods and is consistent with theoretical predictions only to within large uncertainties. A higher top-quark measuring accuracy may be obtained on the e^+e^- collider also by measuring the $t\bar{t}$-pair production cross section near the threshold. The evolution of the theoretical predictions obtained in Ref. [17] is depicted in Fig. 13. As is evident, with an increase in top-quark width, the rise in the cross section in the 1S resonance region becomes less steep.

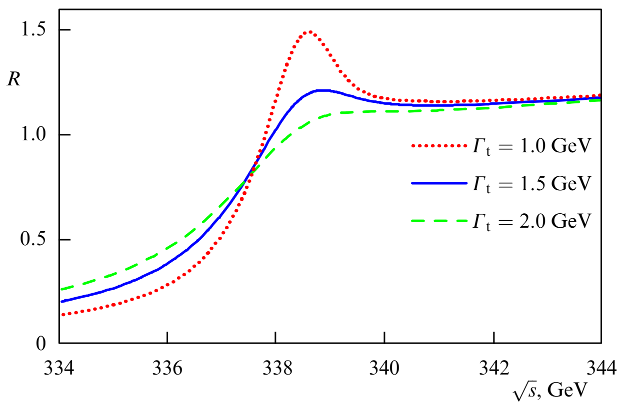

Figure 13. $t\bar{t}$-pair production cross section calculated as a function of e^+e^- collider energy for various top-quark widths and normalized to the value of $\sigma(\mu^+\mu^-)_{QED}$. The simulations assumed the values $m_t = 170$ GeV and α_s (30 GeV) = 0.142.

It is noteworthy that the contribution of the loop diagram with the Higgs boson exchange between top- and anti-top quarks leads to about a 10% increase in the $t\bar{t}$-pair production cross section both at a high energy and near the threshold [17]. Using this property, the $t\bar{t}H$ coupling constant may be indirectly obtained by measuring the $t\bar{t}$-pair production cross section with an accuracy of several dozen percent.

Another important measurement, which can be performed on the linear e^+e^- collider with a much higher accuracy than at the LHC is the top-quark coupling with a Z boson and a photon [3]. On e^+e^- colliders, the $t\bar{t}Z$ and $t\bar{t}\gamma$ vertices participate directly in the leading diagrams of the $e^+e^- \to t\bar{t}$ process and are explicitly included. The vector and axial-vector contributions from $t\bar{t}Z$ and $t\bar{t}\gamma$ vertices may be experimentally separated by accumulating data for different, preferably opposite, beam polarizations and measuring the top-quark production asymmetry A_{FB} and top-quark polarization. As noted earlier, the polarization of the top quark may be measured from the angular distributions of its decay products, since the top-quark decay occurs prior to its hadronization.

Theoretically, measurements of the $t\bar{t}Z$ and $t\bar{t}\gamma$ coupling constants are of the utmost importance, because they may greatly vary among different New Physics models. A significant variation in these quantities is expected among several models of a composite Higgs boson, especially in their versions with additional spatial dimensions. In particular, in the Randall–Sundrum model [49], where additional massive gauge bosons appear ranging in mass from 4 TeV to several dozen TeV, so-called Kaluza–Klein particles or modes, the $t\bar{t}Z$ and $t\bar{t}\gamma$ coupling constants will deviate appreciably from the SM values. The significance of these deviations is estimated at more than 3σ in the acquisition of data with an integrated luminosity of 500 fb^{-1} at an energy of 500 GeV.

There are a number of other important top-quark measurements planned to be made on e^+e^- colliders. The top-quark mass and width may be reconstructed from decay products. A searches for rare top-quark decays is possible for processes with a branching fraction above $10^{-3}-10^{-4}$, depending on the background conditions. This condition is met by the $t \to Ws$ decay, whose search is quite topical. It is also important to measure the top- and anti-top-quark mass differences, which is a test for *CPT* invariance violation.

To summarize the aforesaid, we note that top-quark studies on e^+e^- colliders should be carried out in three total-energy domains. A data set with $L_{int} \sim 100$ fb^{-1} should be accumulated near the $t\bar{t}$-pair production threshold and with L_{int} of at least several hundred fb^{-1} at an energy of ~ 380 GeV, as well as of several hundred fb^{-1} in the domain of three-particle channel opening at an energy of 500–550 GeV.

2.8 Search for New Physics particles

The potential to look for New Physics particles on e^+e^- colliders at an energy of 250 GeV is very limited. If new heavy particles are discovered at the LHC, this would require a reconsideration of the linear collider construction concept in order to achieve higher energies. Nevertheless, a direct search for New Physics particles with a very small coupling to SM particles is possible, and indirect search methods may also be applied. The possible methods for the search for New Physics particles at the ILC intended to verify different theoretical models are described in review Ref. [50]. In this section, we briefly discuss three important measurements which may be carried out at the ILC.

One involves a detailed study of the process $e^+e^- \to f\bar{f}$, where the fermions f are all possible quarks or leptons which may be experimentally reconstructed and identified. Similar to the $e^+e^- \to t\bar{t}$ process considered in Section 2.7, the dominant SM diagrams which describe the $e^+e^- \to f\bar{f}$ processes comprise the vertices $f\bar{f}Z$ and $f\bar{f}\gamma$. In a number of New Physics models, however, deviations from SM values may appear in the measurement of the corresponding coupling constants; these models are reviewed in Ref. [51]. In particular, such deviations may show up in models with new gauge bosons, composite fermions, and additional spatial dimensions. Measurements of such coupling constants were earlier performed on the Large Electron-Positron collider (LEP) and the SLAC [1], but the expected integrated luminosity at the ILC will significantly improve their accuracy. Interestingly, the $b\bar{b}Z$ coupling constants obtained on the LEP are somewhat different from those predicted by the SM [52], and they should be measured more accurately.

A special place among the models of New Physics is occupied by the Z' boson, a heavier analog of the Z boson. In particular, the Z' boson is predicted by different versions of the grand unification theory (GUT) based on the SO(10) group. A searches for the Z' boson has been performed at the LHC, and an upper limit of ~ 3 TeV has been obtained for its mass to date.

On the ILC, the method of extracting the contribution of the heavy Z' boson for the dominant contribution of the vertices $f\bar{f}Z$ and $f\bar{f}\gamma$ is similar to that described in Section 2.7 for the pair top-quark production. It is necessary to measure the process cross sections for different beam polarizations. In this case, the angular distributions of the final states should be studied, preferably at different total energies. In the search for the Z' boson contribution, it is important to perform measurements of the pair production of quarks and leptons with different flavors. As a result of this study at the ILC, under the assumption that the properties of Z and Z' bosons are similar, it will be possible to determine this contribution or rule out a contribution from the Z' boson with a mass up to 5 TeV, and up to 10 TeV in the framework of some models.

The next method in the searches for New Physics at a total energy of 250 GeV is the study of radiative photon spectra. As

[1] The SLAC National Accelerator Laboratory. Prior to 2008: the Stanford Linear Accelerator Center (SLAC).

a result of radiation in the initial state, high-energy photons may be produced, whose spectrum is sensitive to the manifestation of New Physics. By way of example, we mention the searches for weakly interacting massive particles (WIMPs), dark matter particles, proposed in Ref. [53]. Considered in this work is the possibility of searching for the $e^+e^- \to \chi\chi\gamma$ process, in which a WIMP — a particle χ of mass up to 100 GeV — in not recorded by detectors. This approach proposes the use of the method of missing mass to the photon. It is noteworthy that also of interest is the experimental search for monochromatic ISR photons, which may appear in specific models of New Physics.

As with the previous method, the X particles of New Physics of mass in the domain of several dozen GeV may be searched for in the channel $e^+e^- \to ZX$ by analyzing the distribution of the missing mass to the Z boson. This method was employed in LEP experiments, but the sensitivity on the linear collider should be much higher. In recent times, interest has been rekindled in the search for New Physics particles of mass in the area of several dozen GeV and with very small coupling constants. Even for a negative result of the search, this analysis will therefore make it possible to determine limitations for several models of New Physics.

The three reviewed methods for the searches for New Physics may be applied even at an energy of 250 GeV. However, they would work better at higher ILC energies, in particular at 500 GeV. There are also other possible ways of searching for new particles and phenomena on the linear collider, but they will also require an energy above 250 GeV.

2.9 Precision measurements of electroweak theory parameters

Measuring the parameters of the electroweak theory with a high accuracy is a topical problem. Many such measurements have been carried out on the LEP, but there are several reasons why such measurements should be performed at the ILC. First, polarized beams at the ILC open up new possibilities, in particular, for background suppression. Second, the expected integrated luminosity at the ILC is approximately 1000 times higher than in all four LEP experiments. Third, thanks to modern technologies, the ILC detectors will have a significantly higher accuracy: for instance, the momentum resolution of the tracker will improve by one-two orders of magnitude. Fourth, some discrepancy still persists in the combined description of the parameters of the SM, which calls for an improvement of measuring precision.

To study weak processes at the ILC at an energy of 250 GeV, channels with large cross sections are the most convenient: $e^+e^- \to W^+W^-$ and $e^+e^- \to ZZ$. First of all, measurements in these channels will improve the accuracy of measuring the mass, width, and coupling constants of W and Z bosons. It will also be possible to study in detail the structure of γWW and ZWW coupling constants. In many New Physics models, these coupling constants may depart from SM values. One way of introducing New Physics is the EFT formalism, which introduces the tensor formalism, as was done in Eqn (3).

Apart from two-particle channels, also possible is single W boson production in the $e^+e^- \to W^{\pm}e^{\mp}\nu$ channel, but the cross section of this process is small. At a higher energy, it is possible to study channels with three vector bosons: $e^+e^- \to ZW^+W^-$ and $e^+e^- \to ZZZ$. Precise determination of the cross sections for different channels with the production of vector bosons is of importance when estimating the background in the study of other processes, to say nothing of the fact that it is of theoretical significance.

Among the potentially important measurements at the ILC is the precision measurement of the W boson mass. The W boson mass may be accurately measured by accumulating data near the two-particle channel threshold, but at present this option is not being planned. At an energy of 250 GeV it is required to reconstruct the W-boson decay products with the inclusion of kinematic conditions. Systematic inaccuracy will be dominant, since the accumulation of a large number of W bosons will permit a significant lowering of the statistical uncertainty. It is expected that the use of this reconstruction method at the ILC will permit measuring the W-boson mass with an accuracy of several MeV — a level which corresponds to the sensitivity to loop corrections for different New Physics particles [54].

3. Technical aspects of experiments on the e^+e^- collider

As noted in Section 1, presently the base ILC project version comprises a linear e^+e^- collider with a total energy of 250 GeV and two detectors, the ILD and SiD. However, in addition to the base version, there are a number of interesting ideas concerning other e^+e^--collider operating modes. In particular, it is possible to acquire a data set in the region of the Z-boson mass peak which is many times higher than the data set acquired on the LEP. This possibility was discussed at earlier stages of project preparation but was rejected for economic reasons.

There is also a plan to transform the e^+e^- collider into a $\gamma\gamma$ collider. Technically, this may be realized using high-power short-pulse lasers, whose photons scatter from electrons with a large momentum transfer. Such a $\gamma\gamma$ collider will allow carrying out a number of important topical measurements [19]. So far, this option has not been developed further due to resource limitations. Several interesting measurements may be carried out on the e^-e^- collider, and supposedly this will not require substantial modification in construction. The potential of e^+e^--collider development is evident and will undoubtedly be realized.

3.1 ILC collider

A schematic of the ILC accelerator facility proposed in the Technical Design Report (TDR) [1] is depicted in Fig. 14. The collider is designed to operate in the energy range 250–500 GeV and is planned to be 31 km in length. In this case, the possibility of lengthening the collider to 50 km to achieve a total energy of 1 TeV was envisioned at the engineering level. At present, it is being suggested to limit the energy to 250 GeV, which will permit shortening the collider to 20 km. With a decrease in size, the general setup of the accelerator facility remains the same. The proposed particle acceleration scheme is based on 1.3-GHz superconducting radio-frequency technology. The planned collider luminosity should range up to 2×10^{34} cm^{-2} s^{-1}. The TDR implies an average accelerating gradient of 31.5 MeV m^{-1} and a pulse duration of about 1.6 ms. The latest version of the technical project assumes the possibility of increasing the gradient to 35 MeV m^{-1}. The beam energy should be stable to 0.1%.

Electron and positron beams are produced by different techniques. The electron beam is produced with a photocathode polarized source, while positrons are produced by the

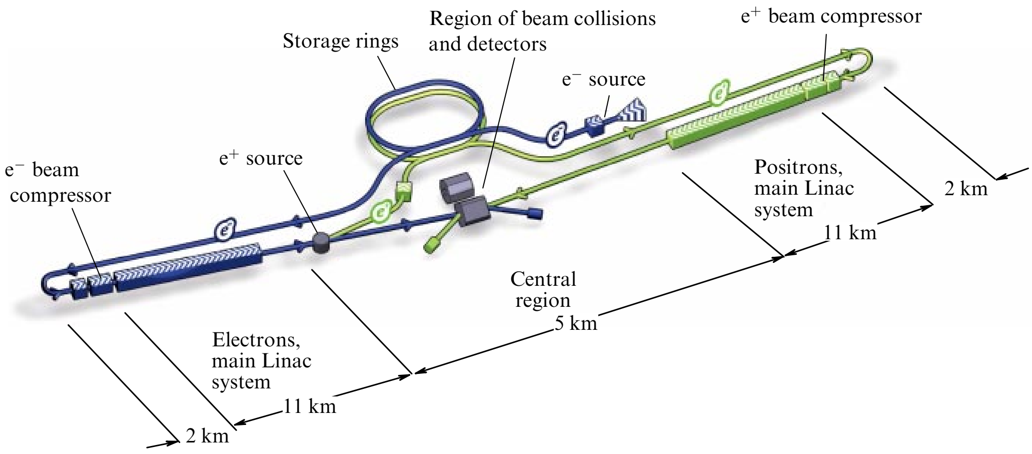

Figure 14. Schematic representation of the ILC facility, which comprises all main subsystems.

in-target conversion of high-energy photons generated in a 147-m-long superconducting helical undulator specially built into the electron beam. Subsequently, the positrons are polarized, cooled, and then injected into a storage ring. The electrons produced in the source are already polarized, their beams also shaped and injected into the electron storage ring. The base version provides for two storage rings, for electrons and positrons at an energy of ~ 5 GeV. Next, the electrons and positrons from the storages rings are fed to the Linear Accelerator (Linac) via a transportation system consisting of a 15-km-long part, which focuses 5-GeV particles and transports them to the point of a 180-degree turn. After the turn, the electrons and positrons are accelerated from 5 to 15 GeV in energy and then arrive at the main Linac system for their final acceleration. The key component, which accelerates the particles to the final energy, is the 11-km Linac system, which consists of superconducting radio-frequency niobium resonators. Upon acceleration, the particles find themselves in the final beam transportation system, where they are additionally focused and collide at the detector center.

In the region of collision, the beams are very small in size, which permits achieving a high luminosity. In this region, the beam measures 5–8 nm vertically and about 0.7 μm horizontally. The beams collide at an angle of 14 mrad. The planned beam currents should be $\sim 5-10$ mA. The e^+e^--collision frequency is expected to be of the order of 5–10 Hz, which permits acquiring data without a trigger system. On reaching the collision point, the beams diverge and decelerate in the damping system.

3.2 ILD detector

The ILD design proposed to date is appreciably different from the ATLAS and CMS detectors mounted at the LHC due to several reasons. The background ILD load will be significantly lighter than for LHC detectors due to the fundamental difference in the operation modes of the e^+e^- and hadron colliders. Owing to the lower energy range of the particles recorded on the ILD, there is no need to construct a giant-sized detector. On the other hand, in the years that elapsed after construction of the LHC, several new state-of-the-art technologies appeared, which were used in the ILD development. This all made it possible to design the ILD with a record high precision of measuring the coordinates of secondary vertices, charged particle momenta, and jet energies.

Figure 15 shows the general view of the ILD [2] on the platform and the arrangement of subdetectors in a quadrant [19]. In the detector design, the emphasis was placed on attainment of a high resolution in the reconstruction of

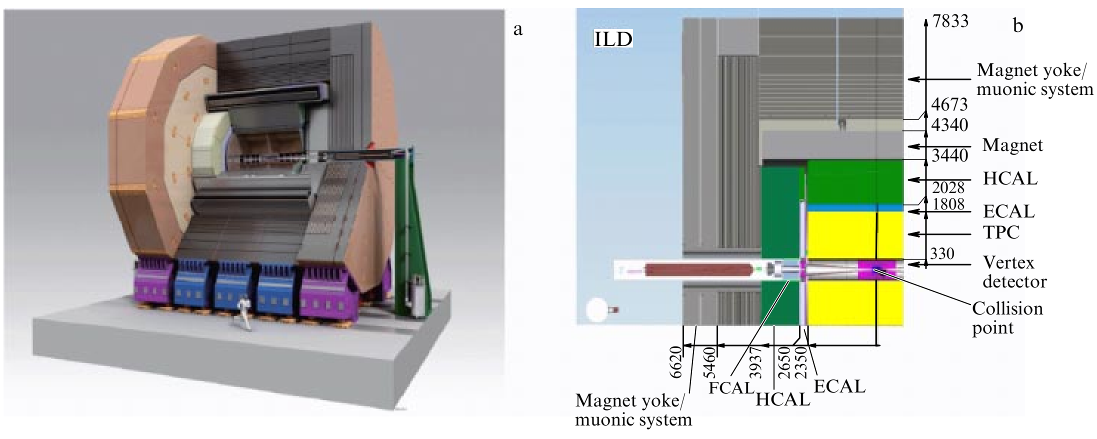

Figure 15. Isometric view of the ILD detector (a) and arrangement of detectors in a quadrant (b). HCAL — hadron calorimeter, ECAL — electromagnetic calorimeter, FCAL — front calorimeter, TPC — time projection chamber. Dimensions are indicated in millimeters.

particles. A substantial effect was exerted by the development of the particle flow algorithm [55] and detector adaptation to the possible use of this method. The ILD has a relatively small size, has no undetected areas or angular intervals, and covers a large angular range.

As is evident from Fig. 15b, nearest to the interaction point is the vertex detector, which is a multilayer pixel semiconductor detector. The vertex detector is important for precision measurements of charged track momenta as a complement to the near-vertex tracker, as well as for high-precision measurements of secondary vertices. The vertex detector must possess a high radiation resistance. With the use of the proposed technologies, the spatial resolution of the vertex detector will be 3–5 μm.

The charged track momenta will be measured with a time projection chamber (TPC), which occupies a relatively large volume in the detector. The camera operation relies on the fact that the resultant ionization clusters drift to its wall, the x and y track coordinates being measured from the projection and the z coordinate from the drift time. This technology permits obtaining a large number of coordinate measurements (up to 224), with the measuring accuracy of each point about 100 μm in all three coordinates. As a result, the tracker has an extremely high resolution in momentum, $\sigma_{1/p_T} = 2 \times 10^{-5}$ GeV^{-1}, approximately 10 times higher than the accuracy of measuring charged particle momenta in the CMS detector. The reconstruction efficiency of tracks with momentum above 1 GeV will be close to 100%. A disadvantage of the time projection camera is its long dead time, but this is not critical for linear collider experiments. The tracker system will be complemented with a stripped silicon detector system arranged behind the TPC, which permits improving the measuring accuracy of track momenta.

The tracker system is surrounded by an electromagnetic calorimeter (ECAL) and further by a hadron calorimeter (HCAL). A special feature of ILD calorimeters is the very high granularity. On the one hand, this provides the possibility of efficiently resolving in the ECAL photons which were produced with close angles. On the other hand, the HCAL will permit achieving a high jet-energy resolution, which is expected at a level $\sigma_E/E \sim 3-4\%$, equivalent to 30% $/\sqrt{E}$ at 100 GeV. Notably, this is of importance for separating Z and W bosons in hadronic decay modes.

It is noteworthy that the high granularity of the calorimeters allows applying the particle flow method, which significantly improves the jet energy resolution. In particular, in the base version of the hadron calorimeter, the cell measures 3×3 cm^2. In the majority of cases, this makes it possible to trace the individual trajectories and energy release of charged particles, even when they are produced in a jet. Therefore, the energy of charged particles emanating from the primary vertex, which is measured in the hadron calorimeter, may be replaced with a quantity obtained by measuring their momentum in the tracker system.

A superconducting magnet coil, which provides an axial magnetic field of 3.5 T in the inner detector part, will be located immediately after the calorimeter. An iron magnet yoke, which is located further, is interlaid with scintillation strip detectors or planar resistive cameras to ensure reliable identification of muons. To date, the final decision between these two technologies has not yet been made.

It is also planned to equip the ILC with a second detector, SiD, which is conceptually slightly different from the ILD. There is only one interaction point in the ILC, and so these detectors will be placed in the beam in turn. It is not unlikely that a decision will be made in the future to use only one detector for economic reasons. In this case, it will be necessary to bring together the best detector technologies developed in both collaborations during the long years of their work.

3.3 Monte Carlo simulations

To perform Monte Carlo simulations of the processes under study and optimize the ILD design, the code package ILCSoft was developed. Data are stored and transferred between the programs of this package in the slcio format. Primary interactions are generated by the Whizard code [56]. Alternatively, for this purpose, use can be made of the CompHEP code [57] developed at Lomonosov Moscow State University (MSU). These programs permit generating different processes at the matrix level, selecting specific intermediate and final states in this case.

Among the important issues of event simulations on the linear collider is the precise inclusion of radiation effects for particle beams like initial-state radiation (ISR), final-state radiation (FSR), and the emission of photons by the particles of one of the colliding bunches in the electromagnetic field of the other bunch (beamstrahlung). These effects may substantially distort the signal shape and result in additional background detector load, especially in the regions close to the beams. The photons are emitted primarily at small angles to the direction of radiating electrons or positrons. When a high-energy ISR photon is emitted, the longitudinal (relative to the beam) momentum component will not be conserved in the event. Mostly the ISR photons do not result in an appreciable violation of momentum conservation in the transverse direction. FSR photons may be emitted in the channel with leptons in the final state, with the result that the signal shape may be distorted in the invariant mass of the particles decaying to leptons.

In the framework of the Whizard package, there are programs that permit simulations of ISR and beamstrahlung effects. FSR is presently simulated using external program products. Unfortunately, the beam configurations in the collision region must be known in detail for the accurate inclusion of radiation effects. At present, beam simulations involve high uncertainties. The presently employed beam model is expected to provide an adequate description of the radiation effects. An example of the radiation effects induced distortion is shown in Fig 5, which shows that the signal shape becomes significantly non-Gaussian on inclusion of these effects in the simulations.

Program-generated primary particles are processed by the detector simulation program DD4hep (Detector description for high energy physics) based on the standard code package Geant-4. In the detector simulation program, the detector geometry may vary, which permits comparing the results of analysis of some process for various detector configurations. Next, data obtained by simulations, which comprise the standard set of subdetector responses, undergo reconstruction using the Marlin program. The same program enables the primary physical analysis of simulation results.

4. Conclusions

This review is a brief consideration of the program of physical research on the linear e^+e^- collider, ILC, at an energy of 250 GeV and above. The ILC project is a thoroughly elaborated plan from the standpoint of collider and detector construction technologies and from the standpoint of the physical research program. It is expected that a decision about ILC construction will be made in the near future. However, even in the case of a negative decision, it will sooner or later be implemented in one country or another, because it is highly demanded. There are inherently similar projects at CERN (CLIC) and in China (CepC), which can pick up the baton from the ILC. As for us, we will hope for the commencement of ILC construction in the near future.

Acknowledgements
The author is grateful to D S Denisov for valuable remarks on the text of the review. This study was supported by the Ministry of Education and Science of the Russian Federation (Government Regulation No. 220, Agreement No. 14.W03.31.0026).

References

1. Adolphsen C et al. (Eds), The International Linear Collider Technical Design Report Vol. 3 (2013); arXiv:1306.6328
2. Behnke T et al. (Eds), The International Linear Collider Technical Design Report Vol. 4 (2013); arXiv:1306.6329
3. Baer H et al. (Eds), The International Linear Collider Technical Design Report Vol. 2 (2013); arXiv:1306.6352
4. Tigner M *Nuovo Cimento* **37** 1228 (1965)
5. Amaldi U *Phys. Lett. B* **61** 313 (1976)
6. Richard F et al., TESLA Technical Design Report; hep-ph/0106314
7. Accomando E et al. (ECFA/DESY LC Physics Group) *Phys. Rep.* **299** 1 (1998)
8. Boos E et al. *Nucl. Instrum. Meth. Phys. Res. A* **472** 100 (2001)
9. Aguilar-Saavedra J A et al. (ECFA/DESY LC Physics Group), hep-ph/0106315
10. Badelek B et al. (ECFA/DESY LC Physics Group) *Int. J. Mod. Phys. A* **19** 5097 (2004)
11. Linssen L et al., arXiv:1202.5940
12. Lebrun P et al., arXiv:1209.2543
13. Dou W et al. *Chinese Phys. C* **37** 097003 (2013)
14. Ruan M et al. *Phys. Rev. Lett.* **112** 012001 (2014)
15. Weiglein G et al. (LHC/LC Study Group) *Phys. Rep.* **426** 47 (2006)
16. Brau J E et al., arXiv:1210.0202
17. Moortgat-Pick G et al. *Eur. Phys. J. C* **75** 371 (2015)
18. Fujii K et al., arXiv:1710.07621
19. Asner D M et al. (ILC Higgs White paper), arXiv:1310.0763
20. Fujii K et al., arXiv:1506.05992
21. Patrignani C et al. (Particle Data Group) *Chinese Phys. C* **40** 100001 (2016), and 2017 update
22. Thomson M A *Eur. Phys. J. C* **76** 72 (2016)
23. de Florian D et al. (LHC Higgs Cross Section Working Group), CERN Yellow Reports: Monographs Volume 2/2017, CERN–2017–002-M (Geneva: CERN, 2017) http://dx.doi.org/10.23731/CYRM-2017-002; arXiv:1610.07922
24. Dürig C et al., arXiv:1403.7734
25. Yan J et al. *Phys. Rev. D* **94** 113002 (2016)
26. Aad G et al. (ATLAS Collab.) *Eur. Phys. J. C* **75** 335 (2015)
27. Khachatryan V et al. (CMS Collab.) *Phys. Lett. B* **736** 64 (2014)
28. Ajaib A, arXiv:1310.8361
29. Barklow T et al. *Phys. Rev. D* **97** 053003 (2018)
30. Gunion J F, Haber H E *Nucl. Phys. B* **272** 1 (1986)
31. Weinberg S *Phys. Rev. D* **13** 974 (1976)
32. Espinosa J R, Grojean G, Muehlleitner M, arXiv:1202.1286
33. Han T, Logan H E, Wang L-T *JHEP* **2006** 099 (2006)
34. Espinosa J R, Grojean C, Muhlleitner M *EPJ Web Conf.* **28** 08004 (2012)
35. Beneke M, Boito D, Wang Yu-M *J. High Energ. Phys.* **2014** 28 (2014)
36. Aad G et al. (ATLAS Collab.) *Phys. Lett. B* **726** 120 (2013)
37. Chatrchyan S et al. (CMS Collab.) *Phys. Rev. Lett.* **110** 081803 (2013)
38. Berge S, Bernreuther W, Spiesberger H *Phys. Lett. B* **727** 488 (2013)
39. Jeans D, Wilson G W *Phys. Rev. D* **98** 013007 (2018)
40. Godbole R M et al. *Eur. Phys. J. C* **71** 1681 (2011)
41. Atwood D et al. *Phys. Rep.* **347** 1 (2001)
42. Kawada S, List J, Berggren M, arXiv:1801.07966
43. Bodwin G T et al. *Phys. Rev. D* **88** 053003 (2013)
44. Vos M, arXiv:1604.08122
45. Marquard P at al. *Phys. Rev. Lett.* **114** 142002 (2015)
46. Vos M, arXiv:1701.06537
47. Seidel K at al. *Eur. Phys. J. C* **73** 2530 (2013)
48. Beneke M et al. *Phys. Rev. Lett.* **115** 192001 (2015)
49. Randall L, Sundrum R *Phys. Rev. Lett.* **83** 3370 (1999)
50. Fujii K et al., arXiv:1702.05333
51. Langacker P *Rev. Mod. Phys.* **81** 1199 (2009)
52. Bagger J A (ed.) (The ALEPH Collab., The DELPHI Collab., The L3 Collab., The OPAL Collab., The SLD Collab., The LEP Electroweak Working Group, The SLD Electroweak and Heavy Flavour Groups) *Phys. Rep.* **427** 257 (2006)
53. Bartels C, Berggren M, List J *Eur. Phys. J. C* **72** 2213 (2012)
54. Baak M et al., arXiv:1310.6708
55. Thomson M A *Nucl. Instrum. Meth. Phys. Res. A* **611** 25 (2009)
56. Kilian W, Ohl T, Reuter J *Eur. Phys. J. C* **71** 1742 (2011)
57. Boos E et al. (CompHEP Collab.) *Nucl. Instrum. Meth. Phys. Res. A* **534** 250 (2004)